GFRP Encasing Efficiency on Enhancement Composite Beams under Static Loading

Fahad M.Bahlol
Department of Civil Engineering, University of Baghdad, Iraq
fahad.abdulkarim2001d@coeng.uobaghdad.edu.iq (corresponding author)

Ali Al-Ahmed
Department of Civil Engineering University of Baghdad, Iraq
dr.ali-alahmed@coeng.uobaghdad.edu.iq

Received: 8 June 2024 | Revised: 14 July 2024 | Accepted: 30 July 2024

 DOI: https://doi.org/10.48084/etasr.8064

ABSTRACT

Structural engineers are increasingly favoring pultruded Glass Fiber-Reinforced Polymer (pultruded GFRP) composite for its lightweight, corrosion resistance, and high strength properties. The utilization of the GFRP material in reinforced concrete structures is not yet well-defined due to a lack of scientific evidence. The study focuses on the structural performance of composite beams made of encased GFRP sections and rebar encased in reinforced concrete. This study highlights the structural significance of embedding GFRP sections in concrete beams composed of GFRP rebars and normal reinforced concrete. To achieve this goal, five different specimens were tested and analyzed under two points of static loading. The experimental program consisted of one reference beam, without the encased GFRP I-section, and four hybrid beams. The study involved installing two types of shear connectors on composite beams with GFRP I-sections to analyze their impact on shear capacity and slide resistance. The experimental findings revealed that encasing the composite beams with GFRP improved their load-bearing and energy dissipation capabilities. Additionally, the shear connectors enhanced the ultimate capacity and eliminated slipping failures. Therefore, there was a strong agreement on the numerical results demonstrating the significance of this work.

Keywords-pultruded GFRP; reinforced concrete; hybrid beam; shear connector

I. INTRODUCTION

Corrosion is a common problem for reinforced structures situated in harsh environmental conditions. Corrosion of steel reinforcing bars causes significant deterioration of concrete structures, resulting in cracks, spalling of the concrete cover, and reduced load-bearing capacity. GFRP materials offer corrosion resistance, electromagnetic neutrality, high strength-to-weight ratios, and high tensile strength, making them a popular choice in the construction sector as a viable alternative to steel [1]. The drawbacks of GFRP reinforcement include: 1) a lower elastic modulus compared to steel, 2) limited ductility (linear-elastic until failure), 3) an ineffective force transfer mechanism (bond system) with the surrounding concrete, 4) concerns regarding serviceability (increased crack width and deflections), and 5) a higher initial cost in comparison to steel reinforcing bars [2]. Encasing the GFRP beam with concrete increases its maximum load and flexibility. Additionally, using shear connectors increases stiffness, thus strengthening the encased beams [3]. The design criteria are mainly about making sure that the top flange of the GFRP profile will still be structurally strong after it has reached its failure load. This is possible with the help of shear connectors, which make a completely bonded connection with the concrete. Hence, the NA's position remains somewhat constant at the same depth [4]. Many researchers have demonstrated how FRP reinforcement affects the serviceability of reinforced concrete beams under flexure [17, 20]. This study is focused on investigating composite beams using GFRP as longitudinal bars and encasing the beam. The main goals of this study are the investigation of the flexural performance of reinforced concrete composite beams with encased GFRP I-sections under static loads, experimentally comparing the composite beams with and without encasing pultruded GFRP sections, the exploration of the efficacy of two shear connector types (Stud and C-channel) on failure mode and slip resistance, and the evaluation of the numerical accuracy of the analyzed data and how close they are to the experimental outcomes.

II. EXPERIMENTAL PROGRAM

Five concrete composite beams were casted and tested under two-point static loading. The specimens had a compressive strength of 30 MPa and were designed with a cross-section of (350*200) mm, an overall length of 3000 mm, a clear span of 2700 mm, and a shear span of 900 mm [13, 14]. The flexural reinforcement comprises five GFRP rebars, with a diameter of 8 mm, two in the compression zone and three in the

tensile zone. Steel stirrups with a diameter of 8 mm and a spacing of 200 mm provide the transverse reinforcement [5, 7]. The longitudinal and transverse reinforcing bars were in accordance with ACI 318-19 [6] to prevent flexural failure and premature shear failure. Table I and Figure 1 illustrate the geometry of the tested specimens and sections, respectively. The reference beam without encased pultruded GFRP I-section is identified by the single label B. Other specimens, which have encased pultruded GFRP I-beam and stud connector, are denoted by the symbols BS, while beams that have had a C-channel connector are denoted by the symbols BC. The distribution of connectors is identified and divided to the symbols T and E. T refers to connectors on top of the beam, when E refers to connectors on the top and bottom of beam. For example, specimen BSTB indicated the composite beam which has encased GFRP I-section with shear stud connectors instilled on top of I-beam. The tested samples were defined by three groups, namely, Reference group, Group F, and Group H. The first group has only a traditional one reinforced concrete beam without an encased section, as shown in Figure (1-a). The second group includes two reinforced concrete composite beams, which have encased pultruded GFRP I-section consisting of two lines of shear connectors instilled on the top of the surface of GFRP section and the difference lies in the connector type. That is, the one was with a stud while the other was with a C-channel, as described in Figure (1-b). Group 2, like group F, contains two suggested composite beams except that it has an additional line of shear connectors fixed to both surfaces of the I-section, as evidenced in Figure (1-c) [18].

TABLE I. MAIN CHARACTERISTICS OF THE COMPOSITE BEAM SPECIMENS

No.	Group	Specimen	Type of encased beam	Connector type	No. lines of connectors
1	Ref.	B	-	-	-
2	F	BSTB	GFRP	Shear Stud	on top
3		BCTB	GFRP	C-Channel	on top
4	H	BSEB	GFRP	Shear Stud	on top and bottom
5		BCEB	GFRP	C-Channel	on top and bottom

III. EST MIXING AND REINFORCED DETIALS

A local company supplied concrete with a 120 mm slump. Cylinders measuring 100 mm in diameter and 200 mm in height were molded and cured in a laboratory tank. The compressive strength results at 7 and 28 days were 20.8 MPa and 30.2 MPa, respectively. The GFRP I-beam, provided by the manufacturer DURA composites in the United Kingdom, was installed at the center of the cross-section [19, 21]. Five 8-mm GFRP rebars for longitudinal reinforcement were included. The steel stirrups had a diameter of 8 mm and a nominal tensile strength of 550 MPa. All stirrups were positioned at a spacing of 200 mm throughout the whole length of the specimens [8]. Additionally, to enhance the connection interface between the GFRP beam and concrete in the compression zone, where concrete lacks strength in tension but does well in compression, two types of steel connectors were used, studs and c-channels. The studs were 80 mm in height and 19 mm in diameter, while the c-channel had dimensions of 75 mm, 50 mm, and 3 mm. The current study specified a minimum of 30 studs with a longitudinal spacing of 200 mm. There are 15 studs for each line and a total of 15 channels for every surface, based on the equivalent steel area of two studs to one channel, as indicated in Figures 5, 8, 9. The laboratory of structural inspections at the college of engineering, Diyala University, conducted tensile testing on material sections and bars in accordance with ASTM A370-14 [10], ASTM D7565/D7565M-10 [11], and ASTM D7205 guidelines [12]. Tables II-V show the characteristics of these groups.

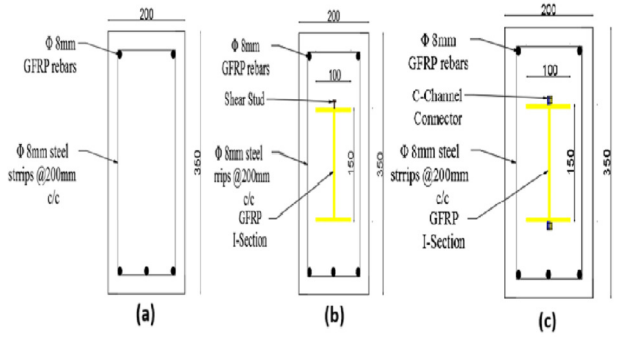

Fig. 1. Details of tested specimens: (a) B- specimen, (b) BSTB – specimen, (c) BCEB- specimen.

TABLE II. TENSILE PROPERTIES OF GFRP BEAMS

Mechanical Properties	Value (MPa)
Transverse Compressive Strength	336
Longitudinal Compressive Strength	305
Longitudinal Tensile Strength	347
Longitudinal Modulus of elasticity	38500
Transverse Modules of elasticity	32200

TABLE III. TENSILE PROPERTIES OF GFRP REBARS

Bar Diameter (mm)	Measured Area (mm^2)	Ultimate Stress (MPa)	Modulus of elasticity (GPa)	Ultimate Load (kN)
8	50.27	1215	55	61

TABLE IV. TENSILE PROPERTIES OF STEEL REINFORCING BARS

Bar Diameter (mm)	Measured diameter (mm)	Yield Stress (MPa)	Ultimate Stress (MPa)	Modulus of elasticity (GPa)
8	7.79	465	598	210

TABLE V. MATERIAL PROPERTIES OF CONNECTORS

Yield Strength (MPa)	Tensile Strength (MPa)	Elongation
346	427	36%

IV. SET UP

Five composite specimens have been tested after their curing for 28 days. They were subjected to two concentrated loads applied at the third point, with a clear span of 2700 mm. They were prepared, cleaned, and painted white to identify and record any possible cracks. The tests were conducted with simply supported beams using a load control system operated by an electro-hydraulic servo universal testing machine with a

capacity of 1000 kN, undergoing a gradual loading procedure [16]. The two point's loads increased gradually at a rate of 5 kN/min. LVDTs were employed to measure the vertical mid-span deflections by placing them under the mid-span surface and at the center of the two horizontal sides to record the slip data between the GFRP beam and concrete. To measure the longitudinal tensile strain of the GFRP rebar and section, a strain gauge was placed on the bottom of the rebar and one on the section. The compressive strain was measured by deploying a separate strain gauge placed on the top of the concrete surface. The pre-wired instruments related to a computerized data acquisition system to automatically collect data during testing. Figure 3 illustrates the dispersion across the composite beams.

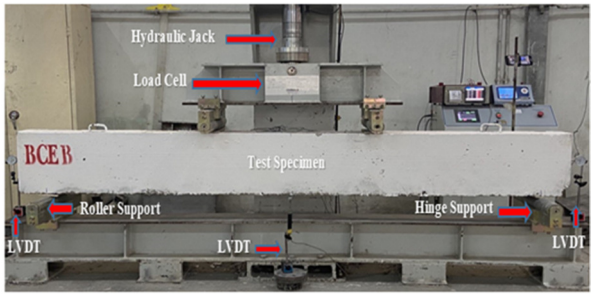

Fig. 2. Details of universal testing machine.

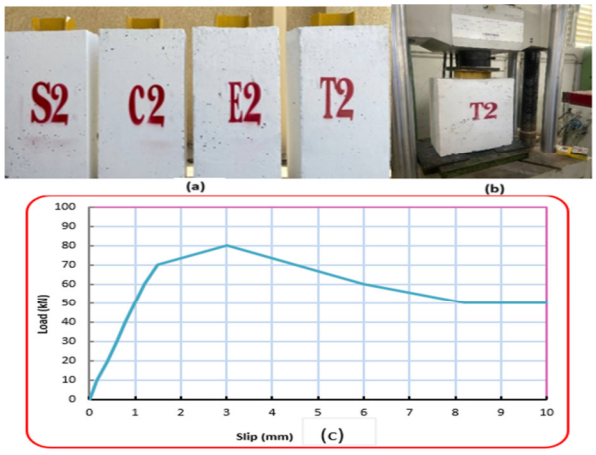

Fig. 3. (a) Experimental specimens, (b) test stage, (c) bond-slip curve.

The bond load slip characteristics between GFRP I- section and concrete were extracted by using the push-out test. The concrete sectional area is 350 mm × 200 mm with a height of 550 mm simulating with the dimensions of the main specimens. Four specimens for this purpose were fabricated and tested in the laboratories, as observed in Figure 3. The results showed slow linearity at the initial loading bond followed approximately by a linear increase in the bond load from this point to the ultimate bond stress, with more substantial slope having been remarked. The end stage experienced a decrease and then climbed again, reaching its maximum bond stress. These experimental data were completely identical with the data of [4].

V. RESULTS

A. Load Deflection

The graphical load-mid-span deflection relationships of five tested beams are shown in Figure 4. The specimens displayed linear elastic behavior in the initial stage, with a high stiffness up to 25% of the ultimate capacity for specimen (B) without GFRP I-section. However, linearity extended to 75% for models with GFRP I-section, showing the strengthening effect of the embedded GFRP beams on the composite specimens compared to the reference beam. This is clear from the load-deflection curves in Figure 3 and the experimental results in Table VI. Composite beams BSTB and BCTB exhibited an 18%–20% rise compared to sample B, whereas specimens BSEB and BCEB displayed a rise of 22%. As the load increased, the deflection in all specimens gradually increased, even after concrete was crushed. However, an obvious change in the linearity of the fourth specimen occurred when the load reached its final level. Non-linear deformation occurs when deflection increases at an earlier rate with a slight increase in load [15]. As the load increased, the tensile GFRP rebars and sections achieved their yield strength. Subsequently, the concrete exhibited crushing in the compression zone, and shear cracks were seen in the shear span during the test. The specimens finally failed in flexure.

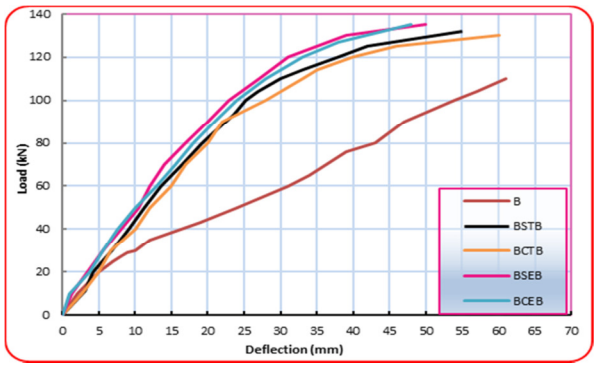

Fig. 4. The Load deflection relationships for tested specimens.

TABLE VI. SUMMARY OF THE EXPERIMENTAL RESULTS

Group	Specimen	Ultimate Load (kN)	Change (%)	Maximum deflection (mm)	Change (%)
Ref.	B	110	-	61	-
F	BSTB	132	20	55	9.84
	BCTB	130	18.18	60	1.64
H	BSEB	135	22.27	50	18.03
	BCEB	135	22.27	48	21.31

B. Load Strain

Two strain gauges were attached to the beams, one on the concrete in the compression zone and the other on the middle GFRP rebar in the tension zone. Figure 5 displays the load-strain curves experimentally obtained for the tested specimens.

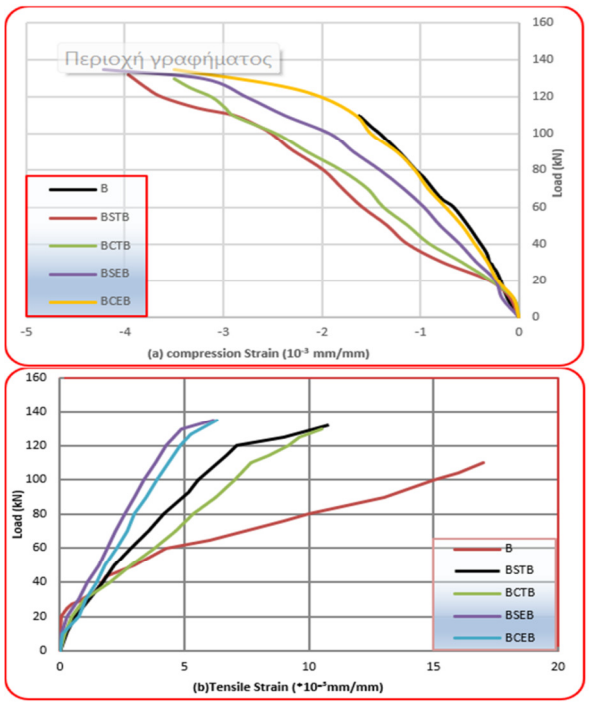

Fig. 5. Load –Strain relationships of the tested specimens.

Positive values are indicated by tensile strains, while negative values are indicated by compressive strains. Specimen (B) exhibited linear strain growth up to 60 kN, reaching a maximum strain value of 0.0016 on the top of the concrete surface. After that, the tensile and compression strains rose, which caused flexural fractures, then the failure of tension rebars, and finally the crushing of the concrete. At a load of 132 kN, the composite beam (BSTB) demonstrated a maximum compressive strain of 0.00396 on the upper concrete surface and 0.00107 on the bottom of the rebar surface. The strain values of the bottom surface of the GFRP rebar increased linearly from the reference beam, indicating that the embedded GFRP section had an impact on the concrete beam's behavior. Subsequently, the strains kept increasing gradually until failure (see also Figure 4). The composite beam (BCTB) with C-channel connectors showed similar performance in both tension and compression zones. The two concrete composite beams (BSEB and BCEB) demonstrated comparable performance, with load-mid-span strain curves indicating higher quality compared to the specimens (BSTB and BCTB). The highest values among these specimens were 0.004 for compression and 0.0062 for tensile. The beams typically collapsed due to GFRP rupture, followed by concrete fracturing. The experimental results revealed that using pultruded GFRP sections significantly improved the structural behavior of composite beams. When loaded with 110 kN, composite beams with one and two surfaces of shear connectors, respectively, had tensile strain reductions of more than 58% and 76% compared to a reference concrete beam without a pultruded GFRP section. Utilizing two surfaces of shear connections significantly reduced the tensile strain approximately by 40% at a load of 130 kN, compared to composite beams with only one surface. In the data response, two distinct types of connectors (stud and C-channel) showed close conduct, lacking distinction. The connector selection is dependent on its qualities.

C. Load Slip

The bond stress-slip relationship was measured at various stages until failure occurred. The horizontal slip between concrete and GFRP I-section was measured by using two LVDTs placed on the side surfaces of composite beams. No slip cracks were discovered on the side surfaces of the specimens, indicating that no slip occurred between the concrete and GFRP beam. Figure 6 displays the crack pattern and failure mode of the composite beams that were tested.

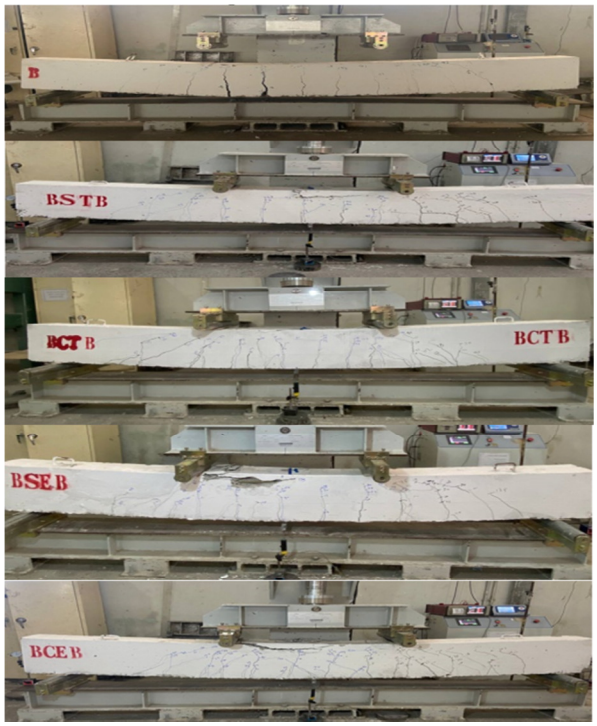

Fig. 6. Crack Pattern at the failure of tested specimens.

VI. CONCLUSIONS

The necessity of innovative/efficient construction sectors to create alternative solutions for traditional problems forces researchers to evaluate and investigate the behavior of? according to suggested structural studies, taking into account the various loads and the surrounding environmental conditions. The significance of using a new FRB profile encased with concrete beams is the base of the current study in an attempt to strengthen its experimental performance and enhance its rigidity, and eventually its contribution to flexural behavior when adopting various types of shear connectors and bonding techniques. Depending on the results of this work, the major conclusions are:

1. Encasing GFRP I-section significantly improves concrete beams' flexural strength and deformation capacity compared to traditional concrete beams.

2. The tensile strain of the GFRP rebars significantly increased linearly up to failure. GFRP beams improved the hybrid beams' strength capability.
3. The specimens (BSTB and BCTB) demonstrate the significance and effectiveness of encasing GFRP sections with concrete, resulting by a 20% and 18.18% increase of the ultimate bearing capacity, respectively. This was accomplished through the incorporation of shear connectors on one surface of the flange beam.
4. Using shear connectors on both the top and the bottom surfaces of GFRP beams increased the peak loads by 22.27% compared to specimen (B). Both types of shear connectors performed equally well on the specimens (BSEB and BCEB) in the test.
5. Utilizing shear connections moderately improved shear resistance control and prevented slide failure by enhancing the composite interface with concrete.
6. Using two surfaces of shear connections on GFRP beams increased the reduction in the deflection data. The decrease was within a range from 18% to 22%, compared to the reference beam.

REFERENCES

[1] Y. Özkılıç, L. Gemi, E. Madenci, and C. Aksoylu, "Effects of stirrup spacing on shear performance of hybrid composite beams produced by pultruded GFRP profle inflled with reinforced concrete," *Archives of Civil and Mechanical Engineering*, vol. 23, Mar. 2023, https://doi.org/10.1007/s43452-022-00576-5.

[2] H. A. Abdalla, "Evaluation of deflection in concrete members reinforced with fibre reinforced polymer (FRP) bars," *Composite Structures*, vol. 56, no. 1, pp. 63–71, Apr. 2002, https://doi.org/10.1016/S0263-8223(01)00188-X.

[3] E. M. Mahmood, A. A. Allawi, and A. El-Zohairy, "Flexural Performance of Encased Pultruded GFRP I-Beam with High Strength Concrete under Static Loading," *Materials*, vol. 15, no. 13, Jan. 2022, Art. no. 4519, https://doi.org/10.3390/ma15134519.

[4] T. H. Ibrahim, A. A. Allawi, and A. El-Zohairy, "Experimental and FE analysis of composite RC beams with encased pultruded GFRP I-beam under static loads," *Advances in Structural Engineering*, Oct. 2022, https://doi.org/10.1177/13694332221130795.

[5] R. P. Johnson, *Composite Structures of Steel and Concrete Beams, slabs, columns, and frames for buildings*, 3rd ed. Blackwell publishing, 2004.

[6] *Building Code Requirements for Structural Concrete (ACI 318-95) and Commentary (ACI 318R-95)*. ACI.

[7] A. M. Ibrahim, W. D. Salman, and F. M. Bahlol, "Flexural Behavior of Concrete Composite Beams with New Steel Tube Section and Different Shear Connectors," *Tikrit Journal of Engineering Sciences*, vol. 26, no. 1, pp. 51–61, Mar. 2019, https://doi.org/10.25130/tjes.26.1.07.

[8] F. M. Bahlol, A. M. Ibrahim, W. D. Salman, and H. A. Abdulhusain, "Effect of Steel Tube Thickness on Flexural Behavior of Concrete Composite Beams Using Different Section Shapes," *Diyala Journal of Engineering Sciences*, pp. 41–49, Dec. 2019, https://doi.org/10.24237/djes.2019.12404.

[9] M. Khalaf and A. Ebid, "Strength Characteristics Of Handy Lay-Up Gfrp I-Beams," *International Journal of Scientific and Engineering Research*, vol. 8, pp. 819–825, Sep. 2017.

[10] *Standard Test Methods and Definitions for Mechanical Testing of Steel Products*. ASTM International.

[11] *Standard Test Method for Determining Tensile Properties of Fiber Reinforced Polymer Matrix Composites Used for Strengthening of Civil Structures*. ASTM International, 2017.

[12] *Standard Test Method for Tensile Properties of Fiber Reinforced Polymer Matrix Composite Bars*. ASTM International, 2006.

[13] P. Kumar and A. Kumar, "Bending Analysis of Steel-Concrete Composite Beams with Porosity," *Engineering, Technology & Applied Science Research*, vol. 13, no. 4, pp. 11230–11234, Aug. 2023, https://doi.org/10.48084/etasr.6050.

[14] M. A. E. Zareef, "An Experimental and Numerical Analysis of the Flexural Performance of Lightweight Concrete Beams reinforced with GFRP Bars," *Engineering, Technology & Applied Science Research*, vol. 13, no. 3, pp. 10776–10780, Jun. 2023, https://doi.org/10.48084/etasr.5871.

[15] T. H. Ibrahim, I. A. S. Alshaarbaf, A. A. Allawi, N. K. Oukaili, A. El-Zohairy, and A. I. Said, "Theoretical Analysis of Composite RC Beams with Pultruded GFRP Beams subjected to Impact Loading," *Engineering, Technology & Applied Science Research*, vol. 13, no. 6, pp. 12097–12107, Dec. 2023, https://doi.org/10.48084/etasr.6424.

[16] A. H. A. Al-Ahmed, A. H. Al-Zuhairi, and A. M. Hasan, "Behavior of reinforced concrete tapered beams," *Structures*, vol. 37, pp. 1098–1118, Mar. 2022, https://doi.org/10.1016/j.istruc.2022.01.080.

[17] A. Hussein Ali Al-Ahmed, A. Al-Rumaithi, A. A. Allawi, and A. El-Zohairy, "Mesoscale analysis of Fiber-Reinforced concrete beams," *Engineering Structures*, vol. 266, Sep. 2022, Art. no. 114575, https://doi.org/10.1016/j.engstruct.2022.114575.

[18] M. I. Ali, A. A. Allawi, and A. El-Zohairy, "Flexural Behavior of Pultruded GFRP–Concrete Composite Beams Strengthened with GFRP Stiffeners," *Fibers*, vol. 12, no. 1, Jan. 2024, Art. no. 7, https://doi.org/10.3390/fib12010007.

[19] T. H. Ibrahim, A. A. Allawi, and A. El-Zohairy, "Impact Behavior of Composite Reinforced Concrete Beams with Pultruded I-GFRP Beam," *Materials*, vol. 15, no. 2, Jan. 2022, Art. no. 441, https://doi.org/10.3390/ma15020441.

[20] M. R. Khalaf, A. H. A. Al-Ahmed, A. A. Allawi, and A. El-Zohairy, "Strengthening of Continuous Reinforced Concrete Deep Beams with Large Openings Using CFRP Strips," *Materials*, vol. 14, no. 11, Jan. 2021, Art. no. 3119, https://doi.org/10.3390/ma14113119.

[21] M. I. Ali, A. A. Allawi, and A. El-Zohairy, "Flexural Behavior of Pultruded GFRP–Concrete Composite Beams Strengthened with GFRP Stiffeners," *Fibers*, vol. 12, no. 1, Jan. 2024, Art. no. 7, https://doi.org/10.3390/fib12010007.